THE JOURNAL OF COMPARATIVE NEUROLOGY 453:22–32 (2002)

Increased Brain Size and Glial Cell Number in CD81-Null Mice

ELDON E. GEISERT, JR.,[1]* ROBERT W. WILLIAMS,[1] GRACE R. GEISERT,[1] LIYING FAN,[1] ANDREW M. ASBURY,[1] HOLDEN T. MAECKER,[2] JUN DENG,[2] AND SHOSHANA LEVY[2]

[1]Department of Anatomy and Neurobiology, and Neuroscience Institute, University of Tennessee, Health Science Center, Memphis, Tennessee 38163

[2]Department of Medicine, Division of Oncology, Stanford University Medical Center, Stanford, California 94305

ABSTRACT

A key issue in the development of the central nervous system (CNS) is understanding the molecular mechanisms regulating cell number. The present study examines the role of CD81 (previously known as TAPA, the target of the antiproliferative antibody) in the control of brain size and glial cell number. CD81 is a member of the tetraspanin family of proteins. This group of small membrane proteins is associated with the regulation of cell migration and mitotic activity. Glial cells express CD81, and antibodies directed against this protein suppress the mitotic activity of cultured cells. In this study, we examine the effects of the CD81 −/− mutation on the CNS of mature mice. These mice have extremely large brains, as much as 30% larger than the brains of wild-type (+/+) littermates. The increase in brain weight is accompanied by an increase in the number astrocytes and microglia, whereas the number of neurons and oligodendrocytes in the CD81 −/− animals appears to be normal. When the CD81 −/− mutation is placed on different genetic backgrounds, there is a remarkable range in the penetrance of the null allele phenotype, demonstrating that the mutation can be affected by modifier loci. This work provides support for the role of CD81 in the regulation of astrocyte and microglial number, perhaps by regulating cell proliferation by a contact inhibition-dependent mechanism. J. Comp. Neurol. 453:22–32, 2002.

Indexing terms: astroglia; microglia; oligodendrocytes; cell number; tetraspanin

The cellular composition of the brain and spinal cord belies a series of molecular events that control the final number of each cell type within the mature central nervous system (CNS). The present study focuses on CD81 (previously known as the target of the antiproliferative antibody TAPA), a small membrane protein that is expressed by all glial cells in the CNS. As its original name suggests, antibodies directed against this protein suppress the mitotic activity of cultured cells (Oren et al., 1990; Geisert et al., 1996). CD81 is a member of the recently defined tetraspanin family of proteins (http://www.ksu.edu/tetraspan/thepage.htm) that is structurally related, with four transmembrane domains and two relatively small extracellular loops (Jennings et al., 1990; Kaprielian and Patterson, 1993; Yatomi et al., 1993; Dong et al., 1995; Kopczynski et al., 1996; Tachibana et al., 1997; Todd et al., 1998; Le Naour et al., 2000; Miyado et al., 2000; Serru et al., 2000). Many of these tetraspanins are found in association with adhesion molecules (Ikeyama et al., 1993; Yanez-Mo et al., 1998; Hemler, 1998; Fitter et al., 1999; Stipp et al., 2001; Charrin et al., 2001). These tetraspanin complexes can link events of cellular adhesion to intracellular signaling cascades (Jennings et al., 1990; Yatomi et al., 1993; Schick and Levy, 1993; Berditchevski et al., 1997). Like other members of

Grant sponsor: PHS; Grant number: RO1 EY12369; Grant number: P30 EY13080; Grant number: CA24233; Grant number: AI45900.

Dr. Maecker's current address is Becton-Dickinson Immunocytometry Systems, 2350, Qume Drive, San Jose, CA 95131.

*Correspondence to: Eldon E. Geisert, Jr., Department of Anatomy and Neurobiology, University of Tennessee, Medical Center, 855 Monroe Avenue, Memphis, TN 38163. E-mail: egeisert@nb.utmem.edu

Received 11 December 2001; Revised 5 April 2002; Accepted 21 June 2002

DOI 10.1002/cne.10364

Published online the week of September 16, 2002 in Wiley InterScience (www.interscience.wiley.com).

this family, CD81 is part of a protein complex within the plasma membrane (Takahashi et al., 1990; Bradbury et al., 1992; Schick and Levy, 1993; Yanez-Mo et al., 1998; Stipp et al., 2001). The specific functional role of CD81 is dependent on its molecular context and the cell type it is associated with. For example, CD81 can be associated with the control of mitotic activity in lymphocytes (Oren et al., 1990), astrocytes (Geisert et al., 1996), or retinal pigment epithelium (Geisert et al., 2002).

In the CNS, CD81 appears to be expressed by all major glial cell classes: ependymal cells, choroid cells, astrocytes, oligodendrocytes (Sullivan and Geisert, 1998), and microglia (Dijkstra et al., 2000). Hints regarding the functional role of this tetraspanin can be gleaned from its dynamic temporal/developmental regulation. During CNS development, neurons are born first and most glial cells are born in a later phase (Caviness, 1982). In this latter phase of brain development, astrocytes and oligodendrocytes are born and mature (Ling and Leblond, 1973; Caviness, 1982; Parnavelas et al., 1983). Most of these cells are born postpartum in the rodent, with peak mitotic activity occurring during the first 10 days (Ling and Leblond, 1973; Parnavelas et al., 1983). By the end of the second postnatal week, astrocytes mature, down-regulate their mitotic activity, and form relatively stable populations (Parnavelas et al., 1983). For oligodendrocytes, the developmental pattern differs from that of the astrocyte. In the second postnatal week, there is an overproduction of oligodendrocytes. Then as myelination occurs, oligodendrocytes undergo an apoptotic cell death if appropriate contacts with axons are not made (Gard and Pfeiffer, 1989; Hardy and Reynolds, 1991). It is during this period of decreased glial mitosis when CD81 is up-regulated dramatically. Relative to the adult, the overall level of this protein increases from 15% at postnatal day (P) 7 to 70% at P14 (Sullivan and Geisert, 1998). This tight correlation of CD81 expression with the down-regulation of glial cell proliferation is consistent with the hypothesis that CD81 plays a role in controlling glial cell number (Sullivan and Geisert, 1998). Based on its apparent function in vitro and its developmental expression pattern, we consider CD81 to be part of a molecular complex regulating glial cell number. To test this hypothesis, we examined the effects of a CD81 −/− mutation on the structure of the adult brain. If this protein is part of the molecular process modulating mitotic activity, then we would predict an increase in the number of glial cells in the brains of CD81 −/− animal and possibly an overall increase in brain size.

MATERIAL AND METHODS

All animal protocols were approved by the Animal Care and Use Committee at the University of Tennessee Health Science Center. Adult mice with a CD81 −/− mutation were produced as previously described (Maecker and Levy, 1997). The original CD81 −/− mutation was carried on a complex genetic background, a mixture of NIHS-BC/Tac and 129X1/SvJ strains. To assess penetrance of the knockout on different genetic backgrounds, we backcrossed carriers to strains with significant differences in brain weight. The −/− mutation was backcrossed to C57BL/6ByJ (average brain weight of ~460 mg) for six generations and onto the small-brain strain BALB/cByJ (average brain weight of ~430 mg) for seven generations. These backcross progeny are >99% homozygous for alleles derived from C57BL/6ByJ and BALB/cByJ. CD81 −/− mice on both inbred backgrounds have difficulty breeding and are propagated as CD81 heterozygotes. We also generated CD81 on a hybrid F1 background by mating BALB/cByJ and C57BL/6ByJ carriers. All mice used in this study were over 70 days of age. We studied male and female mice of all three genotypes. The majority of CD81 −/− animals were females. There are no statistically significant sex differences in brain weights of normal adult mice belonging to any of the three key background strains (129X1/SvJ, C57BL/6ByJ, and BALB/cByJ; data available on-line at www.nervenet.org/main/databases.html, eight cases minimum per sex per strain).

Mice were anesthetized with a mixture of xylazine (13 mg/kg, Rompun) and ketamine (87 mg/kg, Ketalar), which was administered by intraperitoneal injection. The animals were perfused through the heart with a solution of 0.01 M phosphate buffered saline (PBS, pH 7.5) followed by 4% paraformaldehyde in 0.1 M phosphate buffer (PB, pH 7.5). Each brain was removed from the skull, and the spinal cord was separated at a level that corresponds to the decussation of the pyramids. The brains were then blotted dry and weighed on an electronic balance with an accuracy of ± 1 mg.

Brains were placed in a 30% sucrose solution and were sectioned at 50 μm with a freezing microtome. All sections were stored in borate buffered saline (pH 8.4) at 4°C. One 1-in-5 series of sections was mounted on glass slides and stained by the Nissl method. A second series of sections was stained for the astrocytic marker glial fibrillary acidic protein (GFAP). Selected sections from each animal were also stained for the following: (1) a second astrocyte marker using S-100 (Sigma, St. Louis, MO), (2) neurons using NeuN (Chemicon, Temecula, CA), (3) oligodendrocytes using RIP (Chemicon), and (4) microglia using Mac-1 (PharMingen, San Diego, CA). Detailed methods for immunostaining appear in Sullivan and Geisert (1998). The sections were placed in 4% bovine serum albumin (BSA, Sigma) in 0.2 M borate buffered saline (BBS, pH 8.4) for 2 hours, then placed in rabbit anti-GFAP (Immunon) 20 μg/ml in 0.2 M BBS with 1% BSA. Sections were washed 3× for 10 minutes in BBS and transferred to a solution containing the secondary antibody (a peroxidase-conjugated donkey anti-rabbit immunoglobulin G (IgG) or anti-mouse IgG (Jackson Immuno Research Laboratories Inc.) for 2 hours at room temperature. Solutions with primary or secondary antibodies also contained either 0.05% dimethyl sulfoxide or 0.05% Triton X-100. The sections were rinsed in 0.2 M BBS, followed by three rinses in 0.1 M PB (pH 7.2), and incubated in a solution containing 1 mg/ml of 3,3′-diaminobenzidine tetrahydrochloride (Sigma) in 0.02 M PB (pH 7.4) and 5 μl/ml of 3% hydrogen peroxide for 15–30 minutes at room temperature. Controls included sections treated in a similar manner with either the omission of the primary antibody or the substitution of a nonimmune mouse IgG1 (ICN).

Cell counts

The present study was undertaken to determine whether there were significant differences in the brains of animals with a CD81 null (−/−) mutation compared with wild-type (+/+) littermates. Several complimentary approaches were used to evaluate the brains from CD81 −/− mice and the control littermates. The use of frozen sections allowed us to identify specific cell types by immunohistochemical methods. However, there is a considerable

amount of shrinkage in the Z-axis (Abercrombie, 1946; Guillery and Herrup, 1997) that complicates stereologic analysis. For this reason, we chose to use both two-dimensional (2D) counting methods (Abercrombie 1946, Method 1) and the von Bartheld modification of the 3D counting method (Williams and Rakic 1988; von Bartheld, 1999) to analyze several brain regions. Results obtained by using these complementary methods all demonstrate a selective effect of the null mutation on glial cell populations, whether in the whole brain, cortex, hippocampus, or corpus callosum.

Method 1. To define numbers of neurons and glia in the cerebral cortex, a modification of the optical disector was used (Williams and Rakic, 1988; West et al., 1991). In this modification, the entire thickness of the section was included in the counting box as described by von Bartheld (1999). We used a systematic random sampling protocol, counting all cells within a counting box ($120 \times 90 \times 50$ μm) that was moved through the thickness of the cerebral cortex. We estimated the density of glial cells and neurons in the frontal cortex immediately rostral to the somatosensory cortex. A single translaminar probe located 2 mm lateral from the midline was sampled. The number of neurons and glia in successive fields were counted, beginning at the pial surface and continuing through the subcortical white matter. Glial cells were recognized by their small size and distinctive nuclear morphology. Neurons were larger and displayed the large pale nuclear morphology with distinctive cytoplasmic morphology. Similar methods were used in counting the number of immunostained (GFAP-positive or S-100 positive) astrocytes. Cell density estimates were corrected by using Abercombie's method (1946) after assessing cell size by category for over 100 cells per category. In sections immunostained for GFAP, S-100, or Mac-1, the entire immunostained cell body was included in the measurements. This cell size measurement was used to correct the potential sampling bias (Abercrombie, 1946). The tissue was photographed by using an Optronics digital camera on a Leitz Orthoplan microscope. The digitized image was analyzed to determine nuclear area by using NIH image 1.62. The area measurement for each nucleus in the sample population was reduced to a mean diameter ($D = [\text{area}/3.14]^{0.5} \times 2$). The true estimate of cell density or cell number was then calculated by using Abercrombie correction method: $N = n (T / T + D)$, where N is the "true" cell number, n is the estimated cell number, T is the section thickness, and D is the diameter of the nucleus.

Method 2. To estimate changes in neuron-glia ratio in the entire mouse brain, we used a systematic random sampling protocol (Howard et al., 1998) with a grid interval of 2 mm across the entire set of slides as described in Williams (2000). Cells in the counting box that extended the full thickness of the section were categorized and counted. The tissue was imaged by using video-enhanced differential interference contrast optics with a 100×1.25 NA oil-immersion objective. Over 100 sample sites were counted per brain to derive mean estimates of neuron-glia ratio for CD81 −/−, +/−, and +/+ mice.

Method 3. The volume and cell numbers in the hippocampus were determined as follows. The sections were photographed by using an Optronics Magnafier digital camera attached to an Olympus SZX12 microscope. Every series of sections included a calibration image. The area of the hippocampus within each section was determined by using NIH Image 1.62 software. This measure included the hippocampal complex, dentate gyrus, and hippocampus. To define the total volume of the hippocampus, the total cross-sectional area of each hippocampus was multiplied by the sampling interval. Cells in the hippocampus were counted by using a systematic sampling protocol and a standard counting box ($120 \times 90 \times 50$ μm). The sections were stained for microglia (Mac-1) and astrocytes (S-100 and GFAP). These samples of cell densities were averaged and then multiplied by the total hippocampal volume. Cell sizes were measured, and an Abercrombie correction was applied to each case.

Method 4. To define the number of pyramidal cells in the hippocampus, the total length of the hippocampus (CA1, CA2, and CA3) was measured in each of the 1-in-5 series of sections through the hippocampus. The total area of the pyramidal cell layer was calculated by multiplying the linear distance of the cell layer by the interval between sections (250 μm). The cells were counted by using a procedure similar to that described by Abussad et al. (1999), with the exception that our counting box included the entire thickness of the section (50 μm). We counted the total number of pyramidal cells in four fields (two fields from each of two uniformly selected sections) and estimated the total number of pyramidal cells in the pyramidal cell layer for each hippocampus.

Method 5. The total area of the corpus callosum in the sagittal plane was estimated by reconstructing this structure from coronal sections. To estimate numbers of oligodendrocytes, we sampled two uniformly selected regions—the first immediately above the anterior commissure and the second in the plane of section with the subfornical organ. The counting box was $120 \times 90 \times 50$ μm. Total numbers of oligodendrocytes in all three genotypes were compared within the corpus callosum.

Photography

All photomicrographs were produced by digital photography by using an Optronics Magnafier digital camera and Magnafier Software (Optronics, Golenta, CA). Then final figures were constructed by using Adobe Photoshop version 6.

RESULTS

Brains of CD81 knockout (−/−) mice are larger than either wild-type (+/+) or heterozygote (+/−) littermates (Figs. 1, 2B). This difference is not related to any disproportionate enlargement of the cerebral ventricles but is due to an increase in brain mass. The increase in size is evident in parasagittal sections through the brainstem and cerebellum (Fig. 1). The CNS cytoarchitecture in −/− mice is similar to that of the +/+, with the obvious exception that structures are consistently larger than those of either +/+ or +/− mice (Fig. 1). The cortex is also thicker in the −/− mice (Fig. 3). Previous studies found no obvious abnormalities in other organ systems within the CD81 −/− mice (Maecker and Levy, 1997; Tsitsikov et al., 1997; Miyazaki et al., 1997).

Penetrance of the CD81 null mutation

The large brains of −/− mice were characterized initially in mice that were a mixture of two strains NIHS-BC/Tac and 129X1/SvJ (Fig. 2A). We also observed increased brain size in CD81 −/− mice from an F1 cross

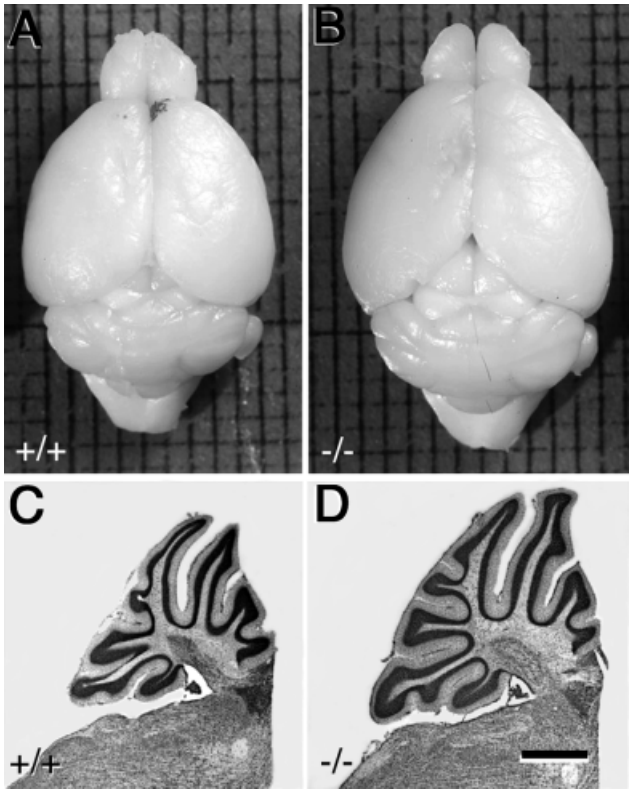

Fig. 1. Effects of the CD81 null mutation on brain size. A dorsal view of brains of +/+ littermate (**A**) and a CD81 −/− mouse (**B**) is shown. Notice the dramatic effect of the CD81 −/− mutation on brain size. The brain of the CD81 −/− mouse weighed 605 mg and was derived from a 26g female, whereas that of the +/+ mouse weighed 463 mg and was derived from a 46-g male mouse. C,D: Parasagittal sections through the brainstem and cerebellum. **C:** A Nissl-stained section from the wild-type mouse shown in A. **D:** A similar section from the littermate with a CD81 −/− mutation shown in B. Notice that the overall structure is similar and that the cerebellum of the CD81 −/− brain is considerably larger than that of the +/+ littermate. Both photomicrographs are taken at the same magnification. Scale bar = 1 mm in D (applies to C,D).

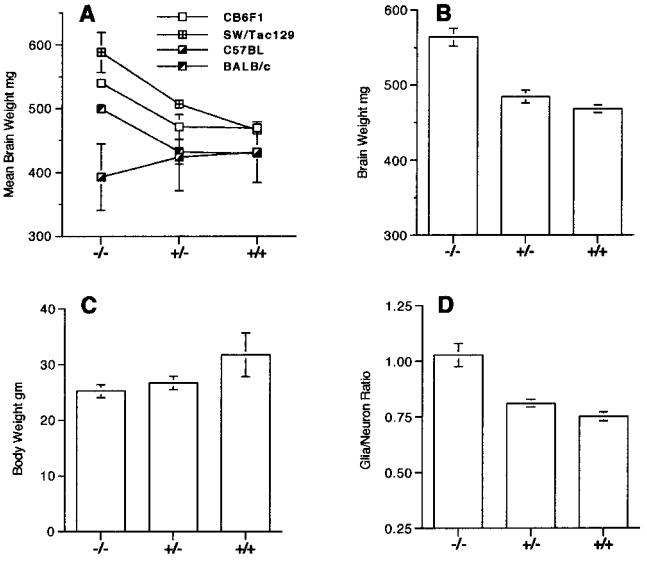

Fig. 2. **A:** The effects of the CD81 −/− mutation on brain weight in four different mouse strains. On mice of a mixed background of NIHS-BC/Tac and 129X1/SvJ mice (SW/Tac 129, n = 9), the CD81 −/− mutation produces very large brains. On the C57BL/6 background (C57Bl, n = 11), there was no difference in brain size between the −/−, +/−, or +/+ mice. The CD81 −/− mutation has an effect on brain size when expressed on a BALB/cByJ background (BALB/c, n = 9). When the CD81 −/− mutation was expressed on an F1 cross between BALB/cByJ mice and C57BL/6 mice (CB6F1, n = 15), the −/− brains were larger than either the +/− or +/+ brains. The results from two backgrounds (F1 BALB/cByJ and C57BL/6; and a mixed background of NIHS-BC/Tac and 129X1/SvJ mice) were combined to illustrate the effect of the −/− mutation on brain weight (B), body weight (C), and glial/neuron ratio (D). **B:** Mean and standard deviation for brain weights (in milligrams) is shown. Brains of CD81 −/− mice are 20% heavier than those of +/− or +/+ mice. There was no difference in the brain weights between the +/− and +/+ animals. This difference in brain weight is statistically significant ($P = 0.0001$, Scheffés F test). **C:** The body weight of the animal is shown. Notice that there is no significant difference between genotypes. **D:** The ratio of glia to neurons in the cerebral cortex is shown. The numbers of glia and neurons were counted in the cerebral cortex of a coronal section. There was a significant increase ($P = 0.005$, Scheffés F test) in the glia to neuron ratio in the −/− mice relative to their +/− and +/+ littermates.

between BALB/cByJ mice and C57BL/6ByJ mice (Fig. 2A). On both of these non-inbred backgrounds, there was an obvious difference between weights of −/− mice and littermates (Fig. 2A). To test the penetrance of the large brain phenotype, we placed the −/− mutation on two different inbred backgrounds, C57BL/By6 or BALB/cByJ (Fig. 2A). Remarkably, when the −/− mutation was introgressed onto the C57BL/By6J background, there was no detectable difference in brain size. When the −/− mutation was placed on a BALB/cByJ background, there was a modest increase in brain size. This important observation demonstrates that the penetrance of the null allele phenotype is dependent on the genetic context. The loss of phenotype on an inbred strain indicates the presence of modifier loci that modulate the effects of the CD81 −/− mutation (Doetschman, 1999).

Analysis of CD81 phenotype

Our detailed analysis of cellular changes that may be targets of the CD81 −/− mutation (Fig. 2B,D) only includes mice with mixed genetic backgrounds—either a mixture of NIHS-BC/Tac and 129X1/SvJ, or F1 crosses of BALB/cByJ mice with C57BL/6ByJ mice. Using these mice with mixed backgrounds eliminates the potential influence of recessive interacting loci. The CD81 −/− mouse brains are, on average, 20% larger than those of either +/+ or +/− littermates (Fig. 2B). This increase in brain size is even more impressive when making comparisons with other strains of mice. The brain weight of CD81 −/− is higher than that of all mice in an extensive database documenting brain weights of over 9,000 mice from 230 strains of genetically defined mice (www.nervenet.org/main/databases.html). No strain had a mean brain weight near that observed in the CD81 −/− animals. The mean brain weight of CD81 −/− animals is 570 mg—three standard deviations higher than that of typical mice. Moreover, no individual mouse in our database has a brain weight greater than 600 mg, whereas two CD81 −/− mice have brains weights over 600 mg. This increase in brain size does not

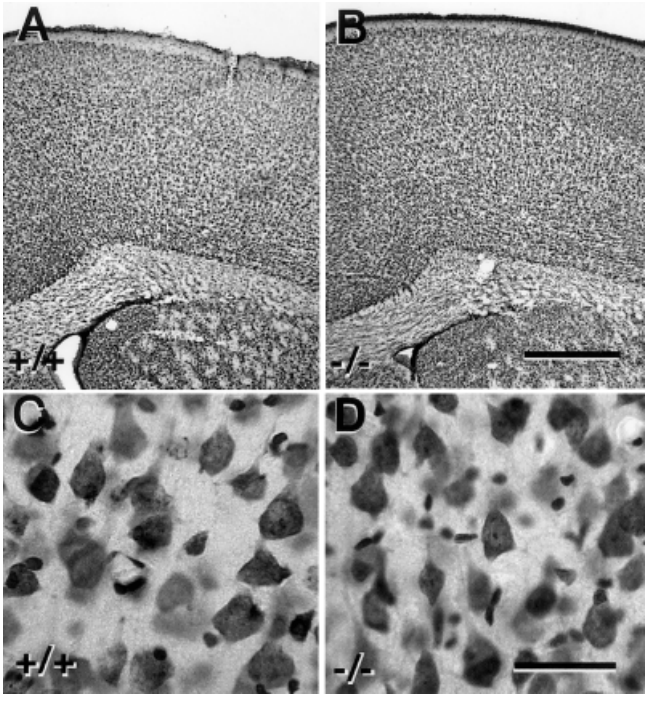

Fig. 3. The effects of CD81 −/− mutation on the histology of the brain is illustrated in Nissl-stained sections. **A:** A photomicrograph from the cortex of a +/+ littermate. **B:** The cerebral cortex from a CD81 −/− mouse is illustrated. The cellular layers in both animals are similar, but the cortex of the CD81 −/− mouse (B) is thicker than that of the +/+ littermate. High-magnification photomicrographs taken from the same cortical region (layer V) are shown for +/+ mice (**C**) and −/− mice (**D**). Scale bar = 500 μm in B (applies to A,B), 100 μm in D (applies to C,D).

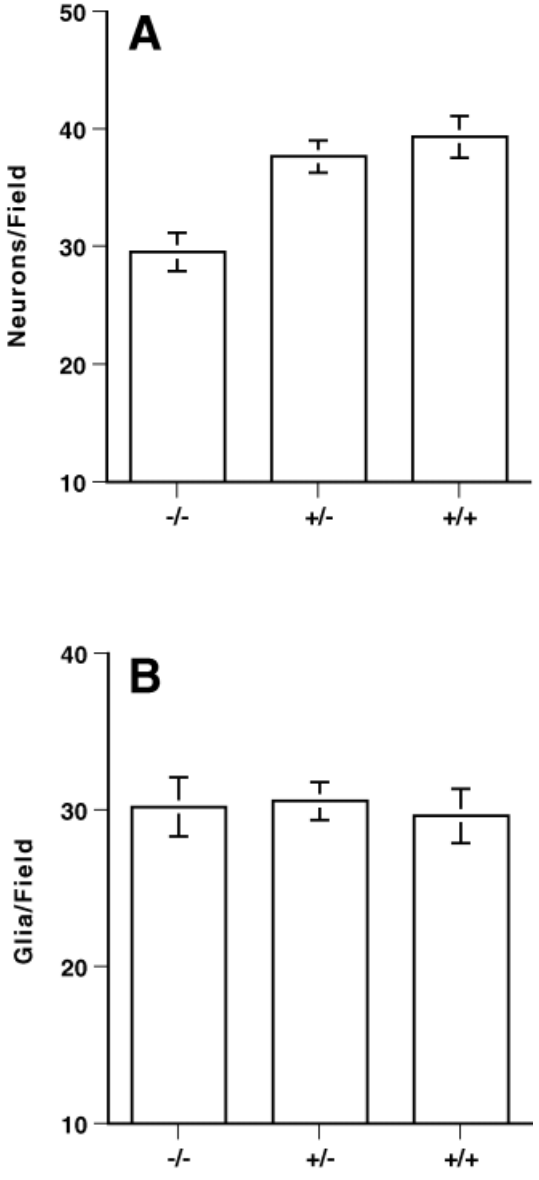

Fig. 4. The density of neurons (**A**) and glial cells (**B**) in the cerebral cortex is shown for each genotype. There is a significant decrease in density of neurons in the cerebral cortex (A; $P = 0.02$, Scheffés F test) but no significant change in the density of glia between −/− mice and +/− or +/+ mice (B). The numbers are expressed in cells/field with each field being 15,950 μ^2.

correlate with either the body weight (Fig. 2C) or sex. These data reveal that the brains of CD81 −/− mice are dramatically larger than those of their +/− and +/+ littermates, or any other strain of mice.

The factors controlling brain size were defined by using a multiple regression analysis with body weight, sex, genetic background, and genotype as independent variables, and brain weight as the dependent variable. The only significant factor controlling brain weight is genotype ($F_{13,4} = 9.8$; $P = 0.0003$). The difference between −/− and +/+ is 103 mg, and genotype alone accounts for 65% of all variance in brain weight in our diverse sample. +/− mice have a normal brain weight, indicating that the −/− has a recessive inheritance pattern on all genetic backgrounds.

To define the basis for this increase in brain size, we estimated the density and numbers of glial cells and neurons (G:N) in Nissl-stained sections. There is a highly significant increase in the G:N ratio in the neocortex of −/− animals (1.09 ± 0.20, Fig. 2D) compared with +/+ (0.78 ± 0.04) and +/− littermates (0.82 ± 0.04). Multiple linear regression using genotype, strain background, brain weight, body size, and sex as dependent variables also demonstrates that only genotype is a significant predictor of the G:N ratio ($P = 0.007$). We also examined densities of glial cells and neurons in Nissl-stained sections. The density of neurons changes dramatically in the different genotype, with the means being 32.2, 39.3, 40.7 neurons/field in −/−, +/−, and +/+ mice, respectively (Fig. 4A). Multiple linear regression using genotype, strain background, brain weight, body size, and sex demonstrates that the only significant predictor of neuron density is brain weight ($P = 0.001$). The brain weight accounts for 71% of the variability in neuron density. Thus, as brains become bigger, the density of neurons decreases, indicating that the total number of neurons within the cerebral cortex of the CD81 −/− mice does not increase proportionately with brain weight. In contrast to the changes in neuronal density, there is virtually no change in the density of glial cells within the different

genotypes. The means from the three groups are 34.5, 32.2, and 31.6 cells/field in −/−, +/−, and +/+ mice, respectively (Fig. 4B). Thus, there is no change in the density of glial cells in the larger brains of the CD81 −/−. The correlate of this finding is that the total number of glia within the brains from the −/− mice is increased relative to that in the +/+ mice.

To assess the effects of the null mutation on the relative densities of neurons and glia throughout the entire brain, a systematic random sampling of the entire brain was conducted. The mean G:N ratio for the entire mouse brain is 1.04 ± 0.03 in −/− animals (n = 3) vs. 0.78 ± 0.02 in +/+ animals (n = 3). These data indicate that the number of glia is increased in the brains of −/− mice, and the larger brains have a decreased neuronal density tending to keep the number of neurons constant.

Effects on the hippocampus

The analysis of the brains from the CD81 −/− mice was extended by examining two well-defined brain structures: the hippocampus and the corpus callosum. As a first step in the analysis, the hippocampus from each animal was reconstructed from Nissl-stained coronal sections to provide an accurate measure of the hippocampal volume (Fig. 5). This analysis revealed that the hippocampus of −/− mice on mixture backgrounds (NIHS-BC/Tac and 129X1/SvJ) have a greater volume than the wild-type littermates. The volume of the hippocampus increased in CD81 −/− mice of F1 cross from BALB/cByJ mice with C57BL/6ByJ mice (Fig. 5A). The hippocampus is slightly larger in the −/− mice when the mutation is placed on the BALB/cByJ background (Fig. 5A). There is no difference in hippocampal volume between the −/− and +/+ mice when the −/− mutation is expressed on the C57BL/By6 background (Fig. 5A). This overall pattern in increased hippocampal volume is very similar to that observed in the changes in brain size (Fig. 2A). The relationship was examined by plotting total brain weight vs. hippocampal volume for each animal (Fig. 5B). This reveals a clear positive correlation between these two measures with a correlation coefficient of 0.82. Thus, the change in hippocampus volume across all genotypes and strains of mice mimic change in the total brain weight.

The number of cell types within the hippocampus was estimated from sections immunostained for astrocytes (GFAP, Fig. 6; S100, Fig. 7E,F), neurons (NeuN Fig. 7A,B), oligodendrocytes and myelin (RIP, Fig. 7C,D), and microglia (Mac1, Fig. 7G,H). The total number of neurons within each hippocampus was estimated by measuring the total linear surface of CA1, CA2, and CA3 of the hippocampus. Neurons were counted in two fields from each hippocampus. These counts of cells were multiplied by the total linear surface of the pyramidal cell layer. The results are shown in Table 1. Notice that there is no significant difference between the number of neurons in the −/− and +/+ mice in both the strains counted. Thus, even though the hippocampus of the −/− mice have a greater volume than the hippocampus of the +/+ mice, there is no significant increase in the number of pyramidal cells. If the volume of the hippocampus has increased and the number of neurons has not, then there must be an increase in the territory of the dendrites of the neurons. To address this specific question, the linear distance from the hippocampal fissure to the alevus was measured in CA1. This distance was measured in four sections through the hip-

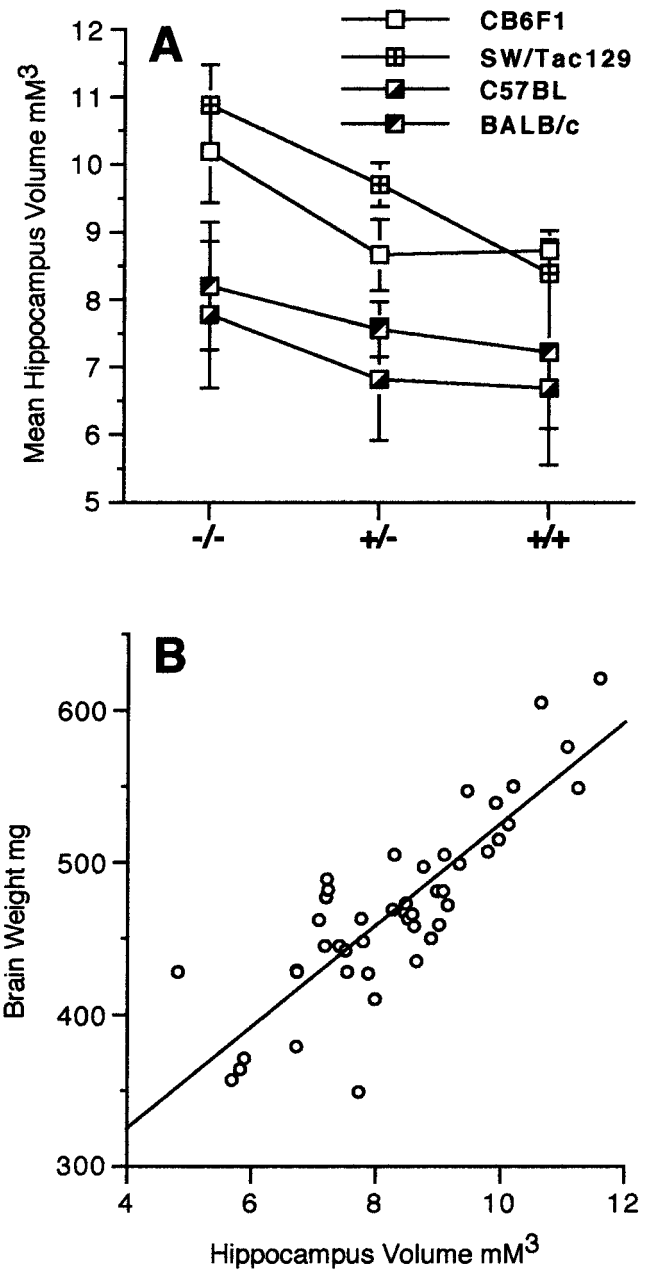

Fig. 5. The volume of the hippocampus (**A**) and relationship to total brain weight (**B**) is shown. The effects of the CD81 −/− mutation on hippocampal volume is shown for four different mouse strains illustrated in Figure 2A. On mice of a mixed background of NIHS-BC/Tac and 129X1/SvJ (SW/Tac 129), mice with the CD81 −/− mutation produce very large hippocampi. When the −/− mutation is expressed on the C57BL/6 (C57Bl) background, there is no difference in hippocampal volume. The CD81 −/− mutation has an effect on the hippocampus when expressed on a BALB/cByJ (BALB/c) background. When the CD81 −/− mutation was expressed on F1 crosses between BALB/cByJ mice and C57BL/6 (CB6F1) mice, the hippocampi were larger than either the +/− or +/+ brains were. The brain weight of each animal was plotted against its hippocampal volume (B). A clear relationship can be observed. Mice with small brains have small hippocampi; whereas animals with large brains have large hippocampi. The regression line is shown, and the correlation coefficient was 0.82.

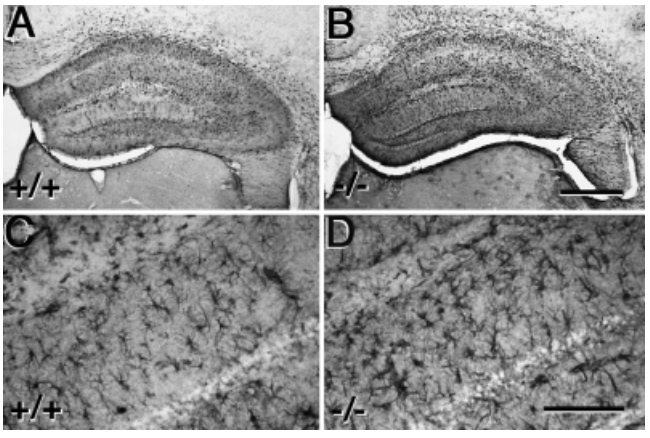

Fig. 6. The distribution of glial fibrillary acidic protein (GFAP) -positive astrocytes in the hippocampus of CD81 −/− (**B**) and +/+ mice (**A**) is shown. All sections were stained in batch, so that each section was exposed to the same concentration of antibodies. The overall intensity of GFAP immunoreactivity is considerably higher in the CD81 −/− animal (B and D). At a higher magnification (C and D) showing the junction of the dentate gyrus and hippocampus, the increased number of astrocytes in the −/− mice can be observed (C is +/+ and D is −/−). C and D are shown at the same magnification. Scale bars = 1 mm in B (applies to A,B), 200 μm in D (applies to C,D).

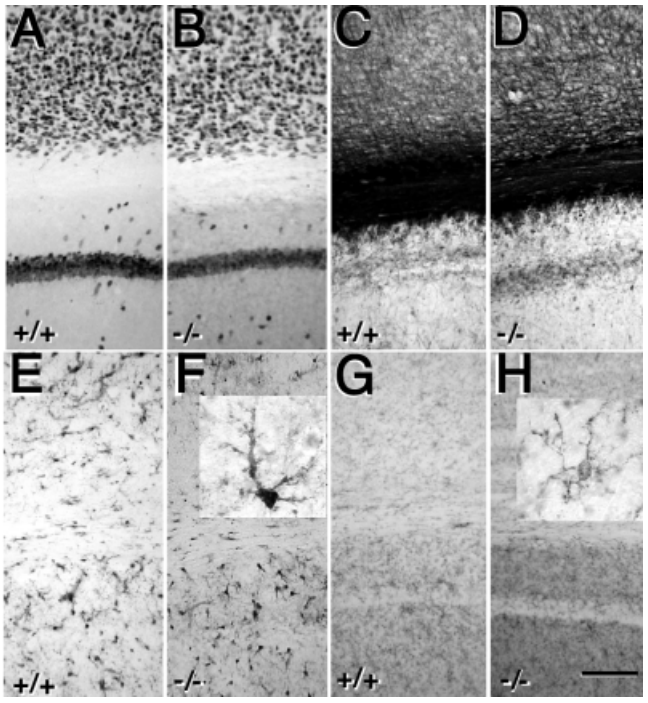

Fig. 7. Sections through the hippocampus from −/− (B,D,F,H) and +/+ (A,C,E,G) mice were stained with antibodies directed against NeuN (**A,B**), RIP (**C,D**), S-100 (**E,F**), and Mac1(**G,H**). The insert in F is a high magnification of a single S-100 stained hippocampal astrocyte. The insert in H illustrates a single Mac-1–positive microglia. Scale bar = 250 μm in H (applies A–H).

pocampus at the level of the habenula, from the −/− and +/+ mice with mixed backgrounds (mixture of NIHS-BC/Tac and 129X1/SvJ and F1 cross from BALB/cByJ mice with C57BL/6ByJ mice). The average distance in the −/− mice was 571 μm (SD = 37 μm), whereas in the +/+ littermates, the average distance was 531 μm (SD = 35 μm). The −/− mice had a 7.5% increase in the thickness of CA1 relative to the normal littermates. This increase was a significant difference ($P < 0.01$; Student t test). Thus, the increase in volume of the hippocampus and the thickness of the hippocampus allows room for a greater expanse of the pyramidal cell dendritic fields in the −/− mice.

When we estimated the total number of astrocytes within the hippocampus, there was a distinct increase in the number of astrocytes in the hippocampus of the CD81 −/− mice compared with their +/+ littermates (Table 1). This increase in astrocyte number was observed in sections stained for GFAP (Fig. 6) as well as sections stained for S-100 (Fig. 7E,F). Thus, there is a significant increase in the number of astrocytes within the hippocampus of the CD81 −/− mice relative to their +/+ littermates. This increase is observed in both the CB6F1 mice and SW/Tac129 mice. The number of GFAP-positive cells in the hippocampus of the CD81 −/− animals is significantly higher ($P = 0.01$ level, Scheffé F test), with an average increase of 64%. Counts of S-100–positive cells revealed an average increase of 38% in the CD81 −/− mice ($P < 0.001$, Scheffé F test). Finally, counts of S-100–positive astrocytes in the cerebral cortex showed a 47% increase in the number of S-100 astrocytes in the animals with a CD81 −/− mutation (data not shown). Thus, in the CD81 −/− mice, there is an increase in the number of astrocytes. This increase in astrocyte number is not associated with an increase in cell body size (Table 2).

CD81 and microglial number

There is also an increase in the total number of microglia within the hippocampus of the CD81 −/− mice compared with +/+ littermates (Table 1). To quantify the microglia, sections were stained with a monoclonal antibody directed against Mac-1 (CD11b). This antibody recognized microglia in CB6F1 mice; however, no cells were stained in the SW/Tac129 mice. When estimates were made for the total number of microglia within the hippocampus, we observed a 58% increase in the number of microglia ($P = 0.001$ level, Scheffé F test).

CD81 and oligodendrocyte number

The final cell type to be examined was the oligodendrocyte. In sections stained for RIP, the myeloarchitecture of the CD81 −/− brains is in general similar to that observed in the CD81 +/+ animals (Fig. 7C,D). The RIP antibody stains both myelin and oligodendrocyte cell bodies. When the sections were examined to count the number of oligodendrocytes, the cell body labeling was obscured by the immunolabeled myelin. Thus, we turned to Nissl-stained sections and the corpus callosum to evaluate potential changes in the overall number of oligodendrocytes. The corpus callosum is an especially well-defined white matter tract. The initial step of our analysis was to reconstruct the cross-sectional area in the sagittal plane of the corpus callosum from coronal sections. For the analysis of the corpus callosum, we examined the CB6F1 mice. Despite a very appreciable difference in brain weight, there was no

TABLE 1. Effects of CD81 −/− on Different Cell Types in the Two Strains of Mice, CB6F1 and Sw/$_{Tac}$.129[1]

	Cell type			
Strain	Neurons/hippocampus	S-100/hippocampus	GFAP/hippocampus	Microglia/hippocampus
CB6F1 −/−	174000 ± 38000	63000 ± 9000	70000 ± 14000	65000 ± 9000
CB6F1 +/+	182000 ± 34000	38000 ± 9000	42000 ± 18000	38000 ± 9000
Sw/$_{Tac}$. 129 −/−	172000 ± 10000	70000 ± 8000	75000 ± 9000	*
Sw/$_{Tac}$. 129 +/+	181000 ± 23000	44000 ± 4000	52000 ± 9000	*

[1]The numbers were derived from counts using stereologic methods and from calculations based on total length, area, and volume of the hippocampus. There was no significant difference in neuronal numbers between the CD81 −/− and the CD81 +/+ mice. There were significant increases ($P < 0.01$, Student's t test) in the number of S-100–positive cells, GFAP-positive astrocytes, and Mac-1–positive microglia. Asterisks indicate that no data were available. GFAP, glial fibrillary acidic protein.

difference in the cross-sectional area between the −/− and +/+ mice. The mean for the CD81 −/− animals (n = 4) was 886,000 μm^2 (SD = 111,000 μm^2); whereas in the wild-type mice (n = 6) was 814,000 μm^2 (SD = 66,800 μm^2). To define the number of oligodendrocytes within the corpus callosum, we counted the number of oligodendrocytes within two identified regions (above the anterior commissure and above the subfornical organ). These counts were used in combination with the cross-sectional area to calculate the total number of oligodendrocytes within a single sagittal section of the corpus callosum. In the CD81 −/− mice, the mean number of oligodendrocytes was 5,080 cells (SD = 1,160), and for the +/+ mice, the mean was 5,430 (SD = 1,250). Thus, there is no increased size in the cross-sectional area of the corpus callosum, and there is no significant increase in the number of oligodendrocytes within the corpus callosum. These data reveal that oligodendrocyte number, unlike that of astrocytes, is not affected by the CD81 −/− mutation. This issue will be considered in detail in the Discussion section.

CD81 is not an imprinted gene

One issue specifically related to CD81 is the potential for imprinting. The portion of chromosome 7 in which CD81 is located in the mouse contains many imprinted genes (Williams et al., 1998) where only one allele is transcribed. In most cases, the promoter of the mother's copy is inactivated by methylation. To examine the possible role of imprinting, we looked at litters in which the mother and father were CD81 +/−. There were no cases in which the +/− offspring had brains as large as the CD81 −/− littermates, indicating that at least one wild-type allele of CD81 was being expressed in every +/− animal. If the normal copy of CD81 from the mother was imprinted (inactivated by methylation of the promoter), then one would expect that animals receiving the null mutation from the father and an imprinted normal copy from the mother would have a +/− genotype and a big brain phenotype. In addition, we had litters where the mother was either +/+ or +/−, and in all cases, there were no +/− littermates with brains as large as the CD81 −/− animals. Thus, in the CD81 transgenic animals, this potential for imprinting does not appear to affect the brain size.

DISCUSSION

Effects of genetic background

In the present study, genetic background had a profound effect on the big brain phenotype of the CD81 −/− mice. A dramatic increase in brain size was observed in the CD81 −/− mice when the mutation was placed on a non-inbred background of 129/SvJ and NIHS-BC/Tac. In contrast, no difference in brain size was found between CD81 −/− and CD81 +/+ when the mutation was placed on C57BL/6ByJ mice. As with other well-documented mutations (for reviews see, Doetschman 1999; Lariviere et al., 2001; Linder, 2001), the genetic background of a mouse can have profound effects on the big brain (CD81 −/−) phenotype. On the C57BL/6ByJ background, there was no increase in brain size in the CD81 −/− mice compared with the +/+ littermates, although a modest increase in brain weight was observed on the BALB/cByJ background. One potential explanation for these background effects is the presence of interacting genetic modifier loci (Doetschman, 1999). If interacting loci are present in inbred strains, then one test for these interacting loci is to cross two different inbred strains, making an animal that is heterozygous at all loci. CD81 +/− BALB/cByJ mice were crossed with CD81 +/− C57BL/6ByJ mice. In these F1 crosses, the brains of the CD81 −/− mice were significantly heavier than either the +/− or +/+ littermates. Thus, in the CD81 −/− mice, genetic background can affect the big brain phenotype and there appears to be loci that are interacting with the CD81 −/− mutation. Future experiments will aid in defining the nature of the interacting loci.

TABLE 2. Effects of CD81 −/− on Cell Size in the Two Strains of Mice, CB6F1 and Sw/$_{Tac}$.129[1]

	Cell diameters in hippocampus			
Strain	Neurons	S-100	GFAP	Microglia
CB6F1 −/−	8.90 ± .50	12.10 ± .20	10.90 ± .30	9.20 ± .20
CB6F1 +/+	8.90 ± .20	11.50 ± .20	10.90 ± .60	8.90 ± .20
Sw/$_{Tac}$.129 −/−	10.80 ± 1.00	10.90 ± .30	12.10 ± .20	*
Sw/$_{Tac}$.129 +/+	10.90 ± .70	10.90 ± .60	11.50 ± .20	*

[1]The numbers were derived from measuring 25 immunostained cells from each animal in the database. There was no significant difference (using a Student's t test, $P < 0.05$) in the volume of any nucleus or cell body measured (neuron, S-100–positive cells, GFAP-positive astrocytes, and Mac-1–positive microglia) between the CD81 −/− and the CD81 +/+ mice. Thus, the CD81 −/− mutation does not affect cell body size significantly. Asterisks indicate that no data were available. GFAP, glial fibrillary acidic protein.

CD81 regulates astrocyte number

As previously noted, the supportive cells of the CNS express CD81. In developing mice, glial cell production peaks approximately 10 days postpartum, and during the second postnatal week, glial cells exit the cell cycle to form a relatively stable cell population (Caviness, 1982). Based on our previous studies (Geisert et al., 1996; Sullivan and Geisert, 1998), CD81 appears to play a role in this down-regulation, because (1) antibodies directed against this protein block cell cycle progression in cultured astrocytes, and (2) the levels of this protein increase as the mitotic

activity of the astrocytes decreases. In the CD81 −/− mice with large brains, there is an increase in the number of astrocytes. Our laboratory has demonstrated that antibodies directed against CD81 can regulate the growth of astrocytes (Geisert et al., 1996). In the mice with non-inbred backgrounds, there was an average increase of 43% in the number of astrocytes (S-100–positive cells and GFAP-positive cells). Taken together, these data demonstrate that CD81 contributes to the molecular mechanism controlling the final number of astrocytes in the adult rodent brain.

There are two potential mechanisms that may explain the increased number of astrocytes in the brains of CD81 −/− mice. The first is decreased cell death. There is evidence that glial cells undergo apoptosis early in development before the second postnatal week (Soriano et al., 1993; Krueger et al., 1995). However, this seems an unlikely mechanism in CD81 −/− mice, for CD81 expression levels are very low before the second postnatal week (Sullivan and Geisert, 1998). The second possible mechanism is an increase in astrocyte cell proliferation. The down-regulation of glial cell mitotic activity that occurs during early postnatal development correlates with the increase in CD81 expression (Sullivan and Geisert, 1998). During the second postnatal week, CD81 is dramatically up-regulated, increasing from 15% of adult levels at P7 to 70% of adult levels at P14 (Sullivan and Geisert, 1998). Thus, astrocytes express CD81 specifically at the stage at which they down-regulate their mitotic activity. Although the CD81 −/− mutation may affect glial apoptosis, we think it is more likely that CD81 is directly involved in down-regulating astrocyte proliferation during the second postnatal week of development.

CD81 regulates microglia number

In addition to observing an increase in the number of astrocytes in the CD81 −/− brains, there was an increase in the number of microglia. An earlier study demonstrated that antibodies directed against CD81 can regulate the growth of microglia (Dijkstra et al., 2001). The microglial cells increase in number in animals with a CD81 null mutation (Table 1). In the mice with non-inbred backgrounds, the number of microglia increased by 50% for the total hippocampus. The increase in number of microglia parallels the increase observed for astrocytes. The increase in cell types appears to account for most of the change in the CD81 −/− mice; however, we cannot rule out the potential contribution of dendrites or axons to the overall increase in brain mass.

CD81 does not affect oligodendrocyte number

The final glial cell type examined was the oligodendrocyte. The corpus callosum was chosen to define the potential changes in oligodendrocyte cell number, for it is a well-delineated structure. This choice allowed for the serial reconstruction of the callosum from coronal sections to provide an accurate estimate of its cross-sectional area. When the cross-sectional area of the corpus callosum from the CD81 −/− mice was compared with that of CD81 +/+ littermates, there was no significant difference between groups, indicating that the area of this white matter pathway was not altered by the CD81 null mutation. Furthermore, systematic measurements demonstrate no difference in the density of oligodendrocytes within the corpus callosum between the CD81 −/− mice and their +/+ littermates. If the area of the corpus callosum for each animal is multiplied by the density of oligodendrocytes, there is no difference between the CD81 −/− mice and their wild-type littermates. Thus, the CD81 null mutation does not appear to alter the number of oligodendrocytes in the mature mouse brain. The lack of effect of the CD81 null mutation on oligodendrocyte cell number may be directly attributed to its developmental history. We know that cultured oligodendrocytes express CD81 (Geisert et al., 1996) and that it is found in isolated CNS myelin (Sullivan and Geisert, 1998). If this is the case, then why is there no effect on cell number in the CD81 −/− mice? CD81 may be playing a different role in oligodendrocytes than it plays in astrocytes. As with many members of the tetraspanin family, CD81 can form different molecular complexes that are cell-type specific and functionally distinct. In tissue culture, once oligodendrocytes differentiate, they exit the cell cycle (Gard and Pfeiffer, 1989; Hardy and Reynolds, 1991). These differentiated oligodendrocytes express high levels of CD81 (Sullivan and Geisert, 1998). If the same is true in vivo, then once the oligodendrocyte phenotype is determined, the cell would no longer be proliferating and its cell cycle would not be affected by a CD81 mechanism. Thus, the number of oligodendrocytes would not be affected by a null mutation of CD81. Finally, the cellular control of oligodendrocyte cell number is well defined and is dependent on contact with developing axons (Burne et al., 1996; Barres and Raff, 1999). During gliogenesis, there is an overproduction of oligodendrocytes. The cells that do not make appropriate contact with axons, forming myelin sheaths, die by apoptosis. Thus, neuron number regulates oligodendrocyte cell number. In the case of the CD81 −/− mice, there is no detectable change in neuron number. If the number of axons that are myelinated determines the final number of oligodendrocytes, then in the CD81 −/− mice, one would expect to see no change in the number of oligodendrocytes relative to the wild-type littermates.

Controlling astrocyte number in development

Several different cellular interactions may contribute to the control of the astrocyte cell cycle in the developing brain. Glial cells are known to interact with neurons and with each other. When neurons contact developing astrocytes, the cells exit the cell cycle (Hatten, 1985). This down-regulation of glial proliferation appears to be associated with a variety of molecular mechanisms. In the cerebellum, the exit of astrocytes from the cell cycle is controlled by the neuronal protein astrotactin (Zheng et al., 1996). Others (Sporns et al., 1995; Amoureux et al., 2000) have shown that N-CAM plays a role in regulating glial proliferation, and N-CAM on neurons can interact with N-CAM on glial cells. Recently, an additional mechanism involving astrocytic CD81 was described (Kelic et al., 2001). The interaction of CD81 on the surface of cultured astrocytes with neurons added to the culture system is also involved in neurons-induced inhibition of astrocytes proliferation. (Kelic et al., 2001). Glial–glial interactions are also known to regulate glial cell cycle. As cultures of glial cells become confluent, they down-regulate their own mitotic activity. One molecule that may be directly involved in the astrocyte–astrocyte interaction is N-CAM. N-CAM, expressed by cultured astrocytes, inhib-

its the mitotic activity of adjacent astrocytes (Sporns et al., 1995). In cultured astrocytes, CD81 also plays a direct role in regulating glial mitotic activity (Geisert et al., 1996). This tetraspanin concentrates at regions of glial–glial cell contact, and antibodies directed against this protein depress the mitotic activity of cultured glial cells (Geisert et al., 1996). The evidence reveals that CD81 is uniquely placed to affect the glial cell cycle, potentially interacting with the different cellular components of the developing brain.

ACKNOWLEDGMENTS

The authors thank Drs. T.S. Nowak and L.F. Eng for their comments on this article. E.E.G., R.W.W., and S.L. received funding from PHS.

LITERATURE CITED

Abercrombie M.1946. Estimation of nuclear population from microtome sections. Anat Rec 94:239–247.

Abusaad I, MacKay D, Zhao J, Stanford P, Collier DA, Everall IP. 1999. Stereological estimation of the total number of neurons in the murine hippocampus using the optical disector. J Comp Neurol 408:560–566.

Amoureux MC, Cunningham BA, Edelman GM, Crossin KL. 2000. N-CAM binding inhibits the proliferation of hippocampal progenitor cells and promotes their differentiation to a neuronal phenotype. J Neurosci 20:3631–3640.

Barres BA, Raff MC. 1999. Axonal control of oligodendrocyte development. J Cell Biol 147:1123–1128.

Berditchevski F, Tolias KF, Wong K, Carpenter CL, Hemler ME. 1997. A novel link between integrins, transmembrane-4 superfamily proteins (CD63 and CD81), and phosphatidylinositol 4-kinase. J Biol Chem 272:2595–2598.

Bradbury LE, Kansas GS, Levy S, Evans RL, Tedder TF. 1992. The CD19/CD21 signal transducing complex of human B lymphocytes includes the target of antiproliferative antibody-1 and Leu-13 molecules. J Immunol 149:2841–2850.

Burne JF, Staple JK, Raff MC. 1996. Glial cells are increased proportionally in transgenic optic nerves with increased numbers of axons. J Neurosci 16:2064–2073.

Caviness VS Jr. 1982. Neocortical histogenesis in normal and reeler mice: a developmental study based upon [3H]thymidine autoradiography. Brain Res 256:293–302.

Charrin S, Le Naour F, Oualid M, Billard M, Faure G, Hanash SM, Boucheix C, Rubinstein E. 2001. The major CD9 and CD81 molecular partner. Identification and characterization of the complexes. J Biol Chem 276:14329–14337.

Dijkstra S, Geisert EE, Gispen WH, Bar PR, Joosten EA. 2000. Upregulation of CD81 (target of the antiproliferative antibody; TAPA) by reactive microglia and astrocytes after spinal cord injury in the rat. J Comp Neurol 428:266–277.

Dijkstra S, Geisert EE Jr, Dijkstra CD, Bar PR, Joosten EA. 2001. CD81 and microglial activation in vitro: proliferation, phagocytosis and nitric oxide production. J Neuroimmunol 114:151–159.

Doetschman T. 1999. Interpretation of phenotype in genetically engineered mice. Lab Anim Sci 49:137–143.

Dong JT, Lamb PW, Rinker-Schaeffer CW, Vukanovic J, Ichikawa T, Isaacs JT, Barrett JC. 1995. KAI1, a metastasis suppressor gene for prostate cancer on human chromosome 11p11.2. Science 268:884–886.

Fitter S, Sincock PM, Jolliffe CN, Ashman LK. 1999. Transmembrane 4 superfamily protein CD151 (PETA-3) associates with beta 1 and alpha IIb beta 3 integrins in haemopoietic cell lines and modulates cell-cell adhesion. Biochem J 338:61–70.

Gard AL, Pfeiffer SE. 1989. Oligodendrocyte progenitors isolated directly from developing telencephalon at a specific phenotypic stage: myelinogenic potential in a defined environment. Development 106:119–132.

Geisert EE Jr, Yang L, Irwin MH. 1996. Astrocyte growth, reactivity, and the target of the antiproliferative antibody, TAPA. J Neurosci 16:5478–5487.

Geisert EE Jr, Abel HJ, Fan L, Geisert GR. 2002. Retinal pigment epithelium of the rat express CD81 (TAPA, the target of the antiproliferative antibody). Invest Ophthalmol Vis Sci. 43:274–280.

Guillery RW, Herrup K. 1997. Quantification without pontification: choosing a method for counting objects in sectioned tissues. J Comp Neurol 386:2–7.

Hardy R, Reynolds R. 1991. Proliferation and differentiation potential of rat forebrain oligodendroglial progenitors both in vitro and in vivo. Development 111:1061–1080.

Hatten ME. 1985. Neuronal regulation of astroglial morphology and proliferation in vitro. J Cell Biol 100:384–396.

Hemler ME. 1998. Integrin associated proteins. Curr Opin Cell Biol 10: 578–585.

Howard MA III, Reed LK, Mirsky R, Abkes BA, Volkov IO. 1998. An integrated multipurpose lesion-making electrode. Neurosurgery 42: 137–142.

Ikeyama S, Koyama M, Yamaoko M, Sasada R, Miyake M. 1993. Suppression of cell motility and metastasis by transfection with human motility-related protein (MRP-1/CD9) DNA. J Exp Med 177:1231–1237.

Jennings LK, Fox CF, Kouns WC, McKay CP, Ballou LR, Schultz HE. 1990. The activation of human platelets mediated by anti-human platelet p24/CD9 monoclonal antibodies. J Biol Chem 265:3815–3822.

Kaprielian Z, Patterson PH. 1993. Surface and cytoskeletal markers of rostrocaudal position in the mammalian nervous system. J Neurosci 13:2495–2508.

Kelic S, Levy S, Suarez C, Weinstein DE. 2001. CD81 regulates neuron-induced astrocyte cell-cycle exit. Mol Cell Neurosci 17:551–560.

Kopczynski CC, Davis GW, Goodman CS. 1996. A neural tetraspanin, encoded by late bloomer, that facilitates synapse formation. Science 271:1867–1870.

Krueger BK, Burne JF, Raff MC. 1995. Evidence for large-scale astrocyte death in the developing cerebellum. J Neurosci 15:3366–3374.

Lariviere WR, Chesler EJ, Mogil JS. 2001. Transgenic studies of pain and analgesia: mutation or background genotype? J Pharmacol Exp Ther 297:467–473.

Le Naour F, Rubinstein E, Jasmin C, Prenant M, Boucheix C. 2000. Severely reduced female fertility in CD9-deficient mice. Science 287: 319–321.

Linder CC. 2001. The influence of genetic background on spontaneous and genetically engineered mouse models of complex diseases. Lab Anim (NY) 30:34–39.

Ling EA, Leblond CP. 1973. Investigation of glial cells in semithin sections. II. Variation with age in the numbers of the various glial cell types in rat cortex and corpus callosum. J Comp Neurol 149:73–81.

Maecker HT, Levy S. 1997. Normal lymphocyte development but delayed humoral immune response in CD81-null mice. J Exp Med 185:1505–1510.

Miyado K, Yamada G, Yamada S, Hasuwa H, Nakamura Y, Ryu F, Suzuki K, Kosai K, Inoue K, Ogura A, Okabe M, Mekada E. 2000. Requirement of CD9 on the egg plasma membrane for fertilization. Science 287:321–324.

Miyazaki T, Muller U, Campbell KS. 1997. Normal development but differentially altered proliferative responses of lymphocytes in mice lacking CD81. EMBO J 16:4217–4225.

Oren R, Takahashi S, Doss C, Levy R, Levy S. 1990. TAPA-1, the target of an antiproliferative antibody, defines a new family of transmembrane proteins. Mol Cell Biol 10:4007–4015.

Parnavelas JG, Luder R, Pollard SG, Sullivan K, Lieberman AR. 1983. A qualitative and quantitative ultrastructural study of glial cells in the developing visual cortex of the rat. Philos Trans R Soc Lond B Biol Sci 301:55–84.

Schick MR, Levy S. 1993. The TAPA-1 molecule is associated on the surface of B cells with HLA-DR molecules. J Immunol 151:4090–4097.

Serru V, Dessen P, Boucheix C, Rubinstein E. 2000. Sequence and expression of seven new tetraspans. Biochim Biophys Acta 1478:159–163.

Soriano E, Del Rio JA, Auladell C. 1993. Characterization of the phenotype and birthdates of pyknotic dead cells in the nervous system by a combination of DNA staining and immunohistochemistry for 5'-bromodeoxyuridine and neural antigens. J Histochem Cytochem 41: 819–827.

Sporns O, Edelman GM, Crossin KL. 1995. The neural cell adhesion molecule (N-CAM) inhibits proliferation in primary cultures of rat astrocytes. Proc Natl Acad Sci U S A 92:542–546.

Stipp CS, Kolesnikova TV, Hemler ME. 2001. EWI-2 Is a major CD9 and

CD81 partner and member of a novel Ig protein subfamily. J Biol Chem 276:40545–40554.

Sullivan CD, Geisert EE Jr. 1998. Expression of rat target of the antiproliferative antibody (TAPA) in the developing brain. J Comp Neurol 396:366–380.

Tachibana I, Bodorova J, Berditchevski F, Zutter MM, Hemler ME. 1997. NAG-2, a novel transmembrane-4 superfamily (TM4SF) protein that complexes with integrins and other TM4SF proteins. J Biol Chem 272:29181–29189.

Takahashi S, Doss C, Levy S, Levy R. 1990. TAPA-1, the target of an antiproliferative antibody, is associated on the cell surface with the Leu-13 antigen. J Immunol 145:2207–2213.

Todd SC, Doctor VS, Levy S. 1998. Sequences and expression of six new members of the tetraspanin/TM4SF family. Biochim Biophys Acta 1399:101–104.

Tsitsikov EN, Gutierrez-Ramos JC, Geha RS. 1997. Impaired CD19 expression and signaling, enhanced antibody response to type II T independent antigen and reduction of B-1 cells in CD81-deficient mice. Proc Natl Acad Sci U S A 94:10844–10849.

von Bartheld CS. 1999. Systematic bias in an "unbiased" neuronal counting technique. Anat Rec 257:119–120.

West MJ, Slomianka L, Gundersen HJ. 1991. Unbiased stereological estimation of the total number of neurons in the subdivisions of the rat hippocampus using the optical fractionator. Anat Rec 231:482–497.

Williams RW. 2000. Mapping genes that modulate brain development: a quantitative genetic approach. In: Goffinet AF, Rakic P, editors. Mouse brain development. New York: Springer. p 21–49.

Williams RW, Rakic P. 1988. Three-dimensional counting: an accurate and direct method to estimate numbers of cells in sectioned material. J Comp Neurol 278:344–352.

Williams RW, Holdener BC, Angel JM, Oakey R, Hunter KW. 1998. Encyclopedia of the mouse genome VII. Mouse chromosome 7. Mamm Genome 8:S136–S159.

Yanez-Mo M, Alfranca A, Cabanas C, Marazuela M, Tejedor R, Ursa MA, Ashman LK, de Landazuri MO, Sanchez-Madrid F. 1998. Regulation of endothelial cell motility by complexes of tetraspan molecules CD81/TAPA-1 and CD151/PETA-3 with alpha3 beta1 integrin localized at endothelial lateral junctions. J Cell Biol 141:791–804.

Yatomi Y, Ozaki Y, Satoh K, Kume S. 1993. Anti-CD9 monoclonal antibody elicits staurosporine inhibitable phosphatidylinositol 4,5-bisphosphate hydrolysis, phosphatidylinositol 3,4-bisphosphate synthesis, and protein-tyrosine phosphorylation in human platelets. FEBS Lett 322: 285–290.

Zheng C, Heintz N, Hatten ME. 1996. CNS gene encoding astrotactin, which supports neuronal migration along glial fibers. Science 272:417–419.